

Supplementary Information

Facile preparation of a lightweight multifunctional interlayer for high performance Li-S battery

Yuan Lei^{a,#}, Zhenyu Zhang^{a,#}, Zhan Lin^a, Samiran Bhattacharjee^b, Chao Chen^{a,*}

^a School of Chemical Engineering and Light Industry, Guangdong University of Technology, Guangzhou 510006, China.

^b Centre for Advanced Research in Sciences (CARS), University of Dhaka, Dhaka 1000, Bangladesh.

These authors contribute equally to this work.

* Corresponding author, E-mail: c.chen@gdut.edu.cn

Experimental section

Preparation of the NC/G composite

In a typical synthesis, 0.631 g melamine and 1.0405 g terephthalaldehyde was dissolved in 31 ml dimethyl sulfoxide. 0.2 g graphene oxide (GO) was then added to the above solution, which was stirred and refluxed at 180 °C under N₂ atmosphere for 3 days. After cooling to the room temperature, the solid product was collected by filtration, washed with excessive acetone, dried in oven, and finally carbonized at 800 °C in N₂ atmosphere for 1 hour to obtain the nitrogen-abundant carbon/graphene composite (NC/G). For comparison, NC was also prepared using the same procedure, except GO was not introduced into the reaction system.

Preparation of NC/G-modified separator

NC/G was dispersed in 50 ml ethanol by ultrasonication for 0.5 hour to form a uniform slurry. Vacuum filtration was conducted to uniformly coat a NC/G layer onto the pristine PP separator. Different loading amount of the NC/G material on the pristine separator, i.e., 0.24, 0.12, 0.08 mg cm⁻², was prepared, respectively.

Lithium polysulfides adsorption and diffusion tests

Li₂S₆ was selected as the representative of lithium polysulfides for the adsorption and diffusion tests. In the glove box, sublimated sulfur (1.6 g) and Li₂S (0.46 g) were mixed in 50 ml DOL/DME solution (volume ratio of 1:1), which was stirred vigorously at 70 °C for 12 hours to obtain a uniform Li₂S₆ solution (0.2 M). The Li₂S₆ solution was then diluted to 2 mM using DOL/DME solution for the adsorption and diffusion tests. The lithium polysulfides adsorption test was conducted as follows: 20 mg NC/G was immersed in 60 μL 2 mM Li₂S₆ solution for 0.5 hour, and the color change of the solution was recorded by camera. The Li₂S₆ solution before and after NC/G treatment were suffered for UV-vis spectroscopy analysis. For the lithium polysulfides diffusion test, the penetration of Li₂S₆ through the separator with or without NC/G interlayer was tested using an H-shaped device containing 2 mM brownish Li₂S₆ solution (left) and transparent DOL/DME solution (right). The color change of the DOL/DME solution was recorded by camera at different time intervals, i.e., 0, 2, 8, and 24 hours, respectively.

Cells assembly and electrochemical measurements

Carbon nanotube (CNT) was used as the sulfur scaffold for the cathode. CNT and sulfur were mixed at a mass ratio of 2:8 for 0.5 hours, and the mixture was treated at 155

°C under argon atmosphere for 12 hours. Then, the CNT@S composite, super P, and PVDF were mixed in NMP solvent at a weight ratio of 7:2:1. After stirring for 12 hours, the slurry was coated on aluminum foil, which was vacuum dried at 60 °C overnight, and cut into circular pieces with a diameter of 14 mm. The sulfur loading is controlled at 1.2 mg cm⁻². Coin cell (CR2032) was assembled in an argon-filled glove box using lithium foil as the anode. 1 M LiTFSI in a DME/DOL (1:1 v/v) with 1 wt. % LiNO₃ solvent was used as the electrolyte. The electrolyte to sulfur ratio (E/S) was controlled at 15 μL mg⁻¹ S. The charge discharge test was carried out on LAND multichannel battery testing system with a voltage window of 1.7-2.8 V. The cyclic voltammetry (CV) and electrochemical impedance spectroscopy (EIS) was measured by CHI760e electrochemical working station in the voltage range of 1.7-2.8 V.

Material characterization

The matter phase is analyzed by X-ray diffraction (XRD) measurement conducted on the RIGAKU miniflex600x-ray diffractometer (CuK α , λ = 1.54059 Å). The valence state, chemical bond and binding energy of elements was analyzed by X-ray photoelectron spectroscopy (XPS) measurement carried out on the Thermo Scientific escalab 250xi model X-ray photoelectron spectrometer. Ultraviolet visible spectra (UV-Vis) were obtained by the perseetu-1900 spectrophotometer. The morphology of materials were obtained by Field emission scanning electron microscope (SEM, Hitachi SU8010) and Transmission electron microscope (TEM, JEOL-JEM 2100 f). Pore properties of materials were analyzed through nitrogen adsorption-desorption measurement using Belsorp Mini (II). Thermogravimetric analysis (TGA) was conducted on NETZZCH-TG209f3 to

determine the content of sulfur in the electrode. The content of nitrogen, carbon and oxygen elements were tested by the TC500 inorganic oxygen nitrogen hydrogen tester.

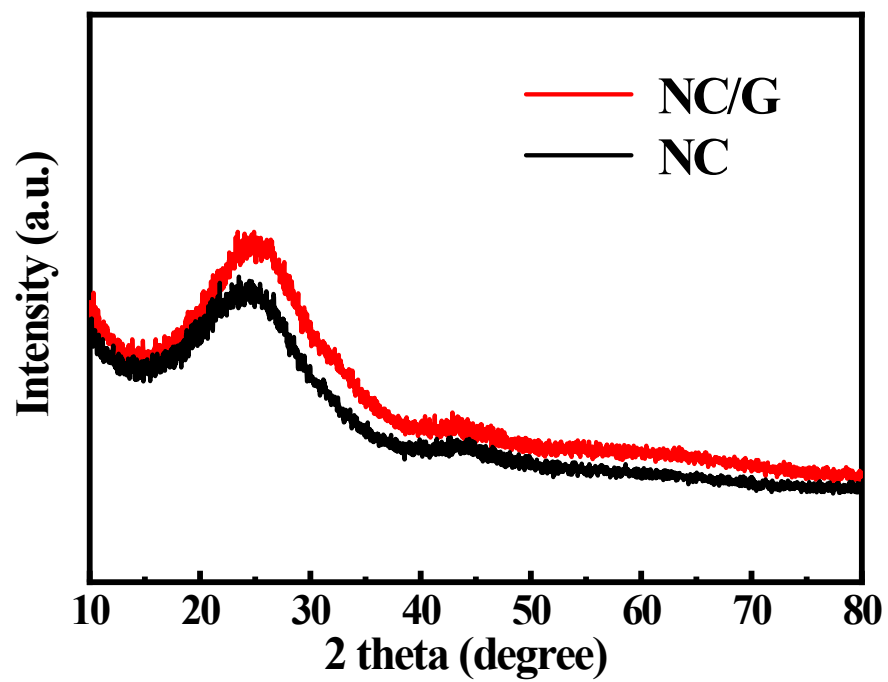


Fig. S1 X-ray powder diffraction patterns of NC and NC/G.

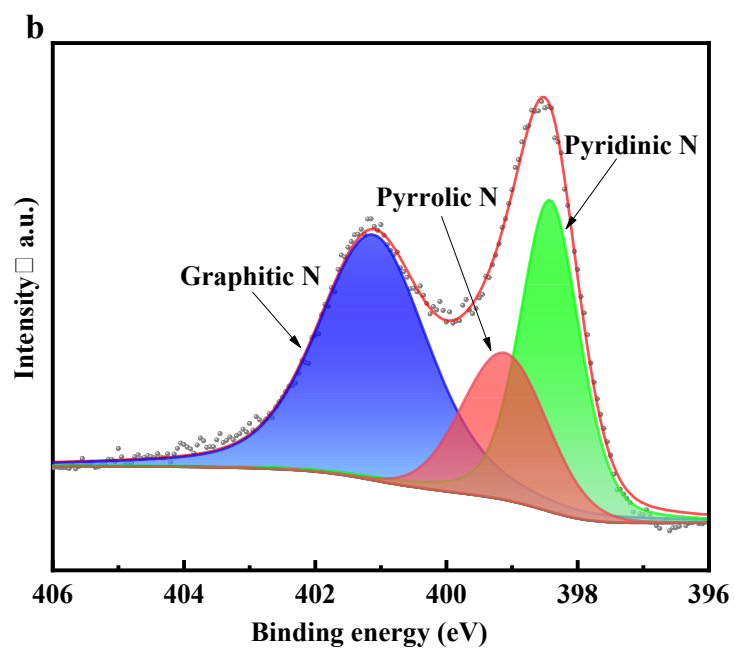
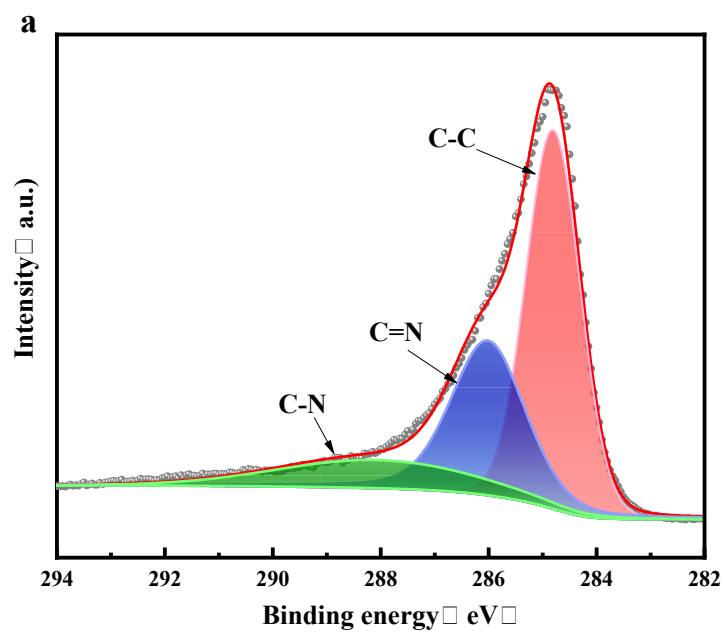


Fig. S2 (a) High-resolution C 1s and (b) N 1s XPS spectra.

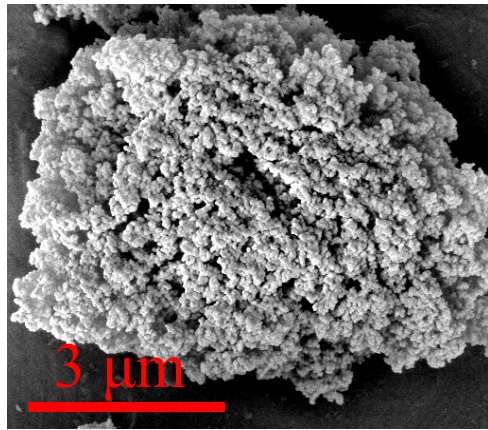


Fig. S3 SEM image of the NC.

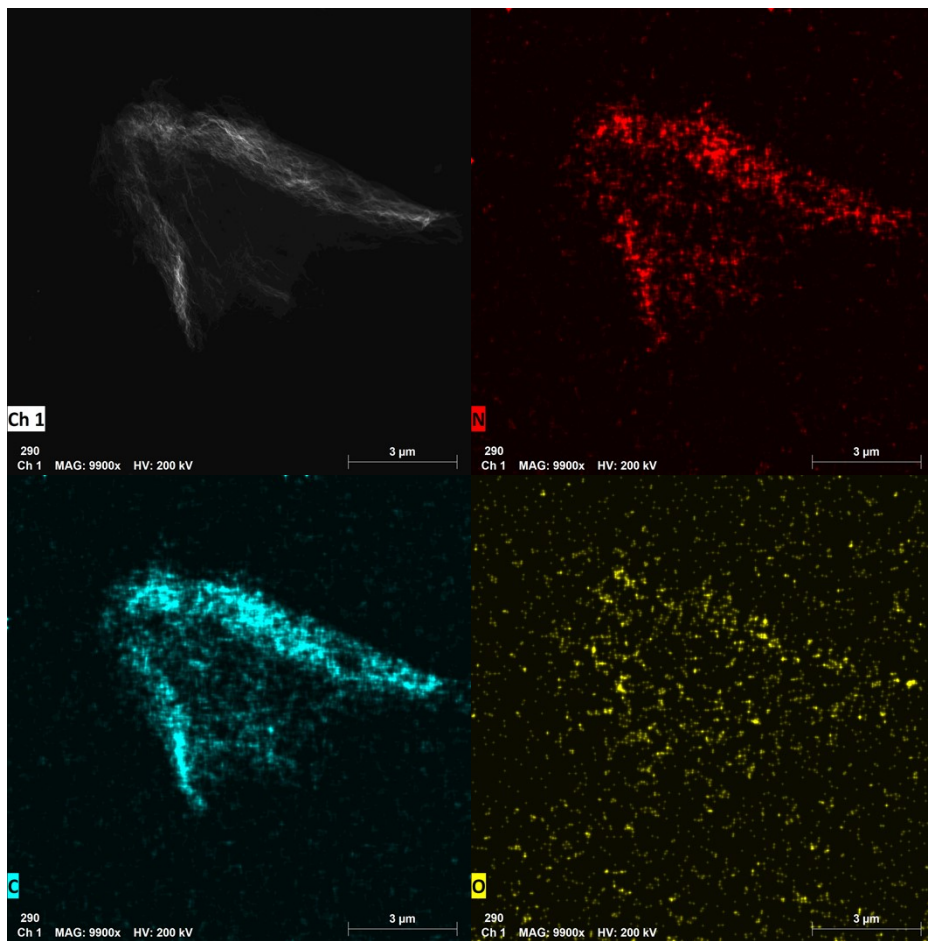


Fig. S4 TEM image of the NC/G.

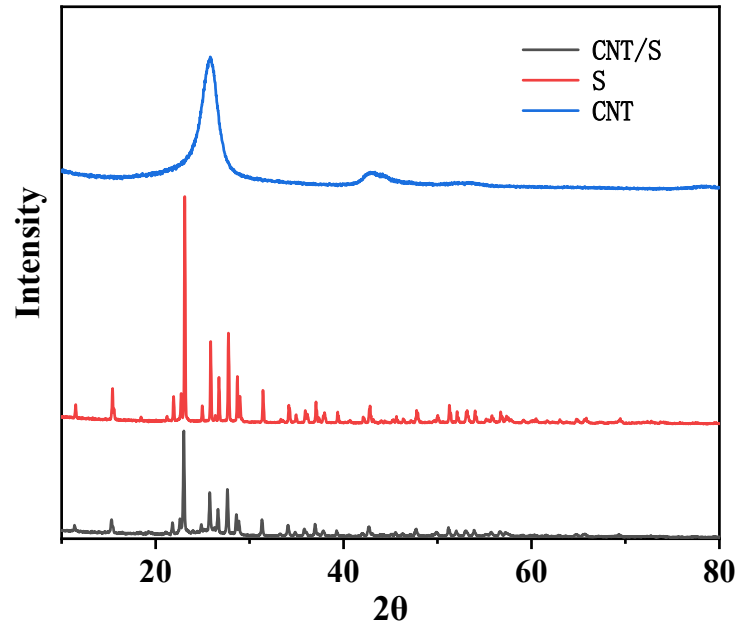


Fig. S5 X-ray powder diffraction patterns of CNS/S composite and pure materials.

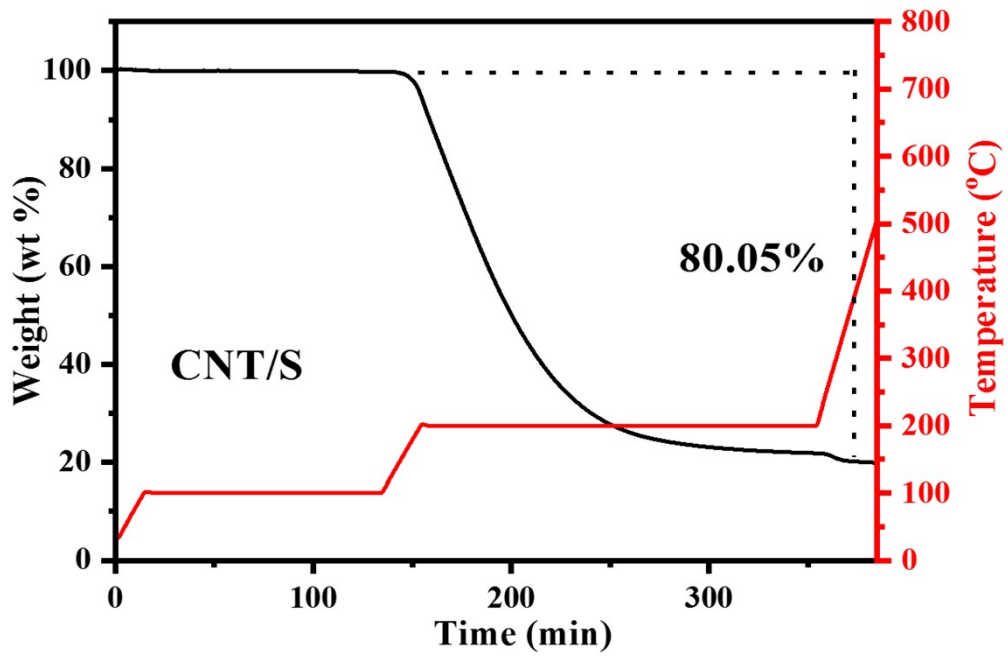


Fig. S6 TGA curves of the S/CNT composite.

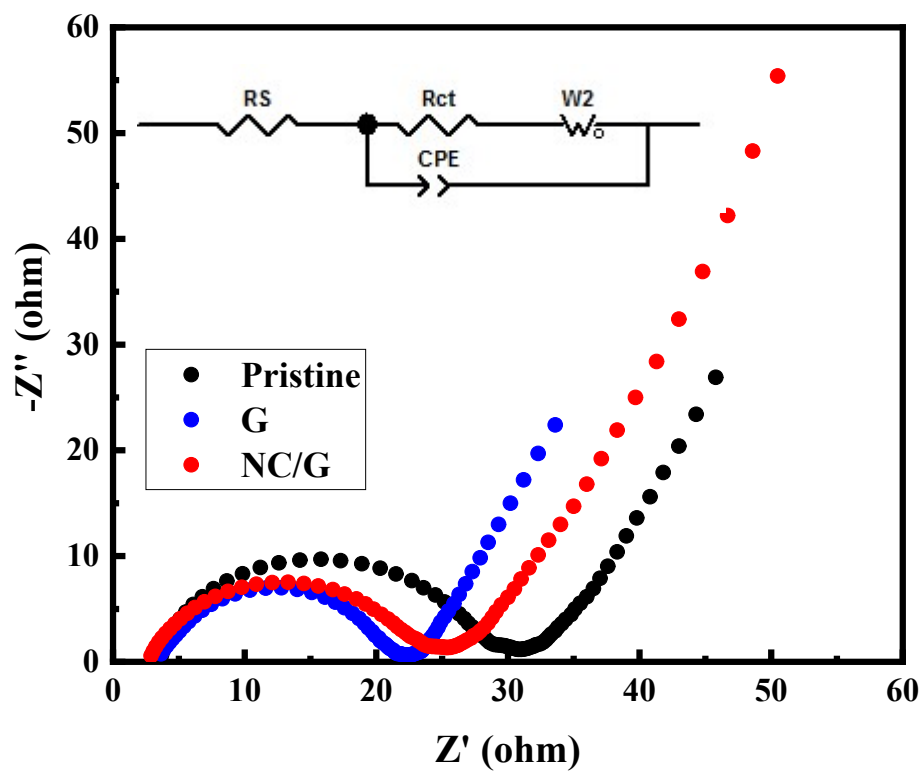


Fig. S7 Nyquist plots of cells assembled with different separators.

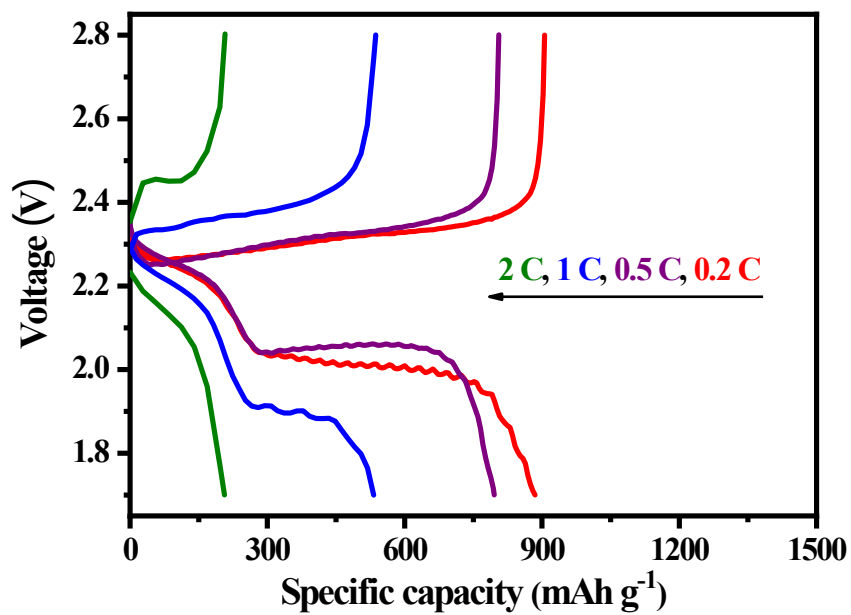


Fig. S8 Galvanostatic discharge-charge profile of the cell assembled with the pristine separator at different current densities.

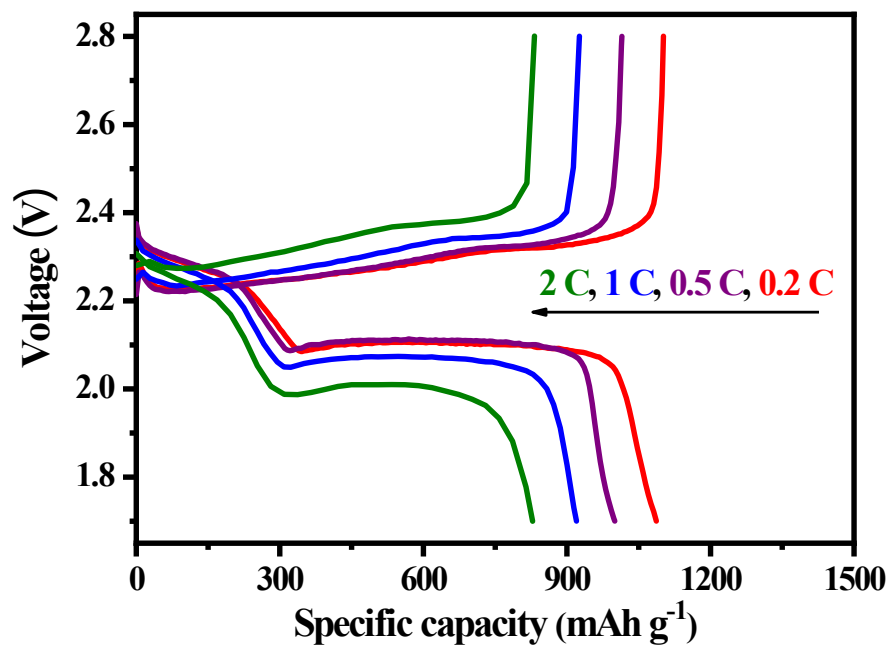


Fig. S9 Galvanostatic discharge-charge profile of the cell assembled with the G-modified separator at different current densities.

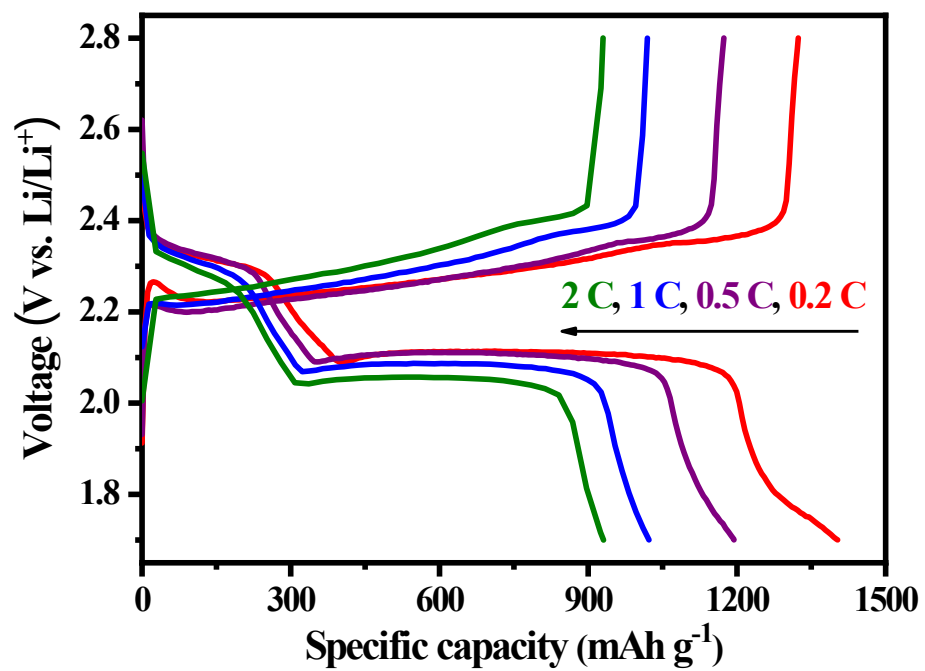


Fig. S10 Galvanostatic discharge-charge profile of the cell assembled with the NC/G-modified separator at different current densities.

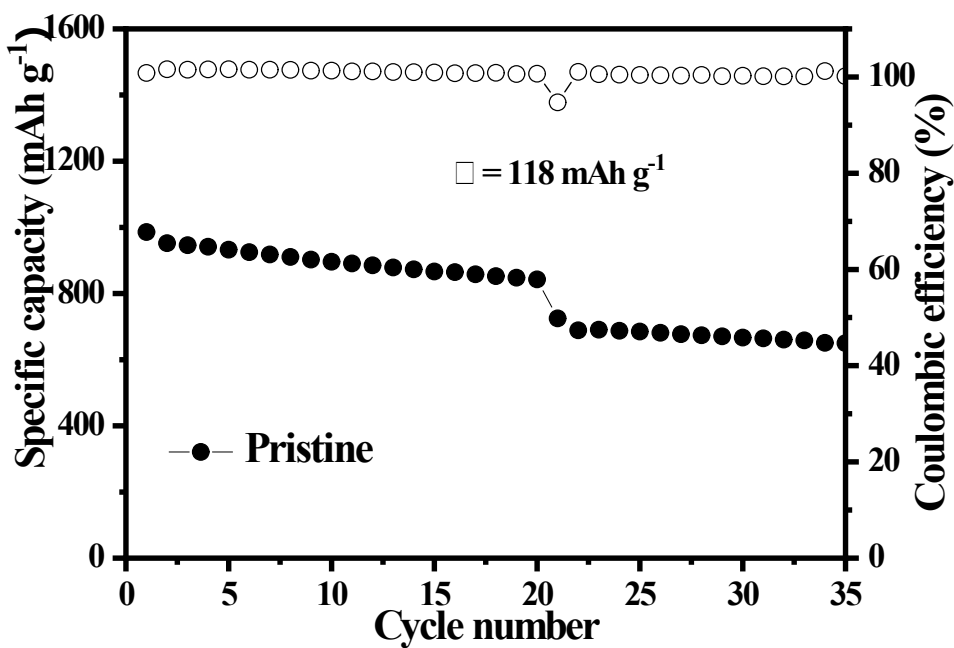
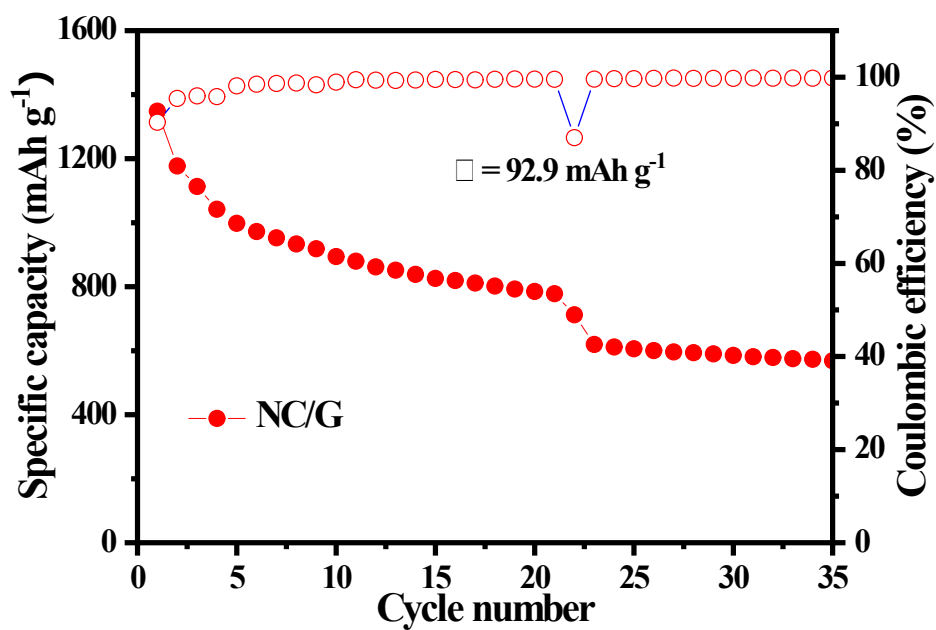


Fig. S11 Cycling performance and capacity decay (5 day rest at 2.1 V during discharge) of batteries with NC/G-modified separator and pristine separator at 0.2 C.

Table S1. Fitting results from EIS.

Separator	$R_s(\Omega)$	$R_{ct}(\Omega)$
NC/G	2.863	19.47
G	3.697	17.08
Pristine	3.592	24.31

Table S2. Physical and chemical characteristics of samples.

Materials	S_{BET} ($m^2 g^{-1}$)	V_{total} ($cm^3 g^{-1}$)	N Content (wt.%)
NC/G	560	0.30	16.2
NC	812	0.39	17.7

Table S3. Comparison of Li-S battery performance assembled with different interlayers with different loading amount of interlayer material on separators.

Interlayer materials	Loading (mg cm ⁻²)	C Rate	Cycle number	Capacity retention (mAh g ⁻¹)	Ref.
Oxygen-doped carbon/rGO	0.5	0.1	200	830	[1]
ZnO nanowire/carbon nanofiber	0.7	1	200	776	[2]
Y-FTZB	1.2	0.25	300	557	[3]
HKUST-1@GO	0.3	0.5	500	799	[4]
Carbon nanofiber/Gum Arabic	0.25	1	250	827	[5]
Porous sulfonated carbon	1.2	0.5	200	776	[6]
Porous-graphene	0.54	0.5	150	877	[7]
PC/MWCNT	0.51	0.5	200	659	[8]
m-Mn ₂ O ₃ /SP	0.3-0.4	0.5	300	553	[9]
P-doped BN/GO	0.1	0.5	500	646	[10]
PW ₄ /Super P	0.25	0.1	70	603	[11]
Se _{0.06} SPAN/MMT	0.5	0.1	300	927	[12]
Zn ₂ W ₂ @2CD	0.28	2	200	659	[13]
FeNi@NC	0.54	0.1	160	836	[14]
SV-VS ₂	0.5	0.2	150	921	[15]
UiO-66(SO ₃ Li) ₄	0.54	0.5	300	874	[16]
Cu SA/N-Ti ₃ C ₂ T _x	0.34	0.2	80	1144	[17]
Ni@NGC	0.1	0.5	200	773	[18]
NSPCF@CoS ₂	0.98	0.5	100	665	[19]
NC/G	0.08	0.5	100	832	This work
	0.24	0.5	100	929	
		1	300	761	
		2	300	720	

Reference

1. L. Zhang, F. Wan, X. Wang, H. Cao, X. Dai, Z. Niu, Y. Wang and J. Chen, *ACS Applied Materials & Interfaces*, 2018, **10**, 5594-5602.
2. T. Zhao, Y. Ye, X. Peng, G. Divitini, H.-K. Kim, C.-Y. Lao, P. R. Coxon, K. Xi, Y. Liu, C. Ducati, R. Chen and R. V. Kumar, *Advanced Functional Materials*, 2016, **26**, 8418-8426.
3. M. Li, Y. Wan, J.-K. Huang, A. H. Assen, C.-E. Hsiung, H. Jiang, Y. Han, M. Eddaoudi, Z. Lai, J. Ming and L.-J. Li, *ACS Energy Letters*, 2017, **2**, 2362-2367.
4. S. Bai, X. Liu, K. Zhu, S. Wu and H. Zhou, *Nature Energy*, 2016, **1**, 16094.
5. S. Tu, X. Chen, X. Zhao, M. Cheng, P. Xiong, Y. He, Q. Zhang and Y. Xu, *Advanced Materials*, 2018, **30**, 1804581.
6. P. J. Kim, H. D. Fontecha, K. Kim and V. G. Pol, *ACS Applied Materials & Interfaces*, 2018, **10**, 14827-14834.
7. P.-Y. Zhai, H.-J. Peng, X.-B. Cheng, L. Zhu, J.-Q. Huang, W. Zhu and Q. Zhang, *Energy Storage Materials*, 2017, **7**, 56-63.
8. L. Tan, X. Li, Z. Wang, H. Guo, J. Wang and L. An, *ChemElectroChem*, 2018, **5**, 71-77.
9. S. J. Park, S. Y. Yang, S. A. Han, Y. J. Choi, T. Kim, M.-S. Park, J. H. Kim and K. J. Kim, *Chemical Engineering Journal*, 2023, **460**, 141620.
10. J. Zhang, W. Ma, Z. Feng, F. Wu, D. Wei, B. Xi and S. Xiong, *Journal of Energy Chemistry*, 2019, **39**, 54-60.
11. W. Yao, L. Liu, X. Wu, C. Qin, H. Xie and Z. Su, *ACS Applied Materials & Interfaces*, 2018, **10**, 35911-35918.
12. W. Wang, K. Xi, B. Li, H. Li, S. Liu, J. Wang, H. Zhao, H. Li, A. M. Abdelkader, X. Gao and G. Li, *Advanced Energy Materials*, 2022, **12**, 2200160.
13. L. Ni, J. Gu, X. Jiang, H. Xu, Z. Wu, Y. Wu, Y. Liu, J. Xie, Y. Wei and G. Diao, *Angewandte Chemie International Edition*, 2023, **62**.
14. Y. Luo, D. Zhang, Y. He, W. Zhang, S. Liu, K. Zhu, L. Huang, Y. Yang, G. Wang, R. Yu, H. Shu, X. Wang and M. Chen, *Chemical Engineering Journal*, 2023, **474**, 145751.
15. L. He, X. Zhang, D. Yang, J. Li, M. Wang, S. Liu, J. Qiu, T. Ma, J. Ba, Y. Wang and Y. Wei, *Nano Lett.*, 2023, **23**, 7411-7418.
16. S. Lin, J. Dong, R. Chen, G. Zhang, T. Huang, J. Li, H. Zhou, L.-H. Chung, X. Hu and J. He, *Journal of Alloys and Compounds*, 2023, **965**, 171389.

17. H. Gu, W. Yue, J. Hu, X. Niu, H. Tang, F. Qin, Y. Li, Q. Yan, X. Liu, W. Xu, Z. Sun, Q. Liu, W. Yan, L. Zheng, Y. Wang, H. Wang, X. Li, L. Zhang, G. Xia and W. Chen, *Advanced Energy Materials*, 2023, **13**, 2204014.
18. N. Baikalov, I. Rakhimbek, A. Konarov, A. Mentbayeva, Y. Zhang and Z. Bakenov, *RSC Advances*, 2023, **13**, 9428-9440.
19. N. Wu, J. Wang, C. Liao, L. Han, L. Song, Y. Hu, X. Mu and Y. Kan, *Journal of Energy Chemistry*, 2022, **64**, 372-384.